INVITED PAPER

Near-field optical investigations of photonic crystal microresonators

B. C. BUCHLER[†], **P. KRAMPER**[††], **M. KAFESAKI**[†††], **C. M. SOUKOULIS**[†††,††††], ***and*** **V. SANDOGHDAR**[†a)],

SUMMARY We present an overview of our work on the application of scanning near-field optical microscopy (SNOM) to photonic crystal structures. Our results show that SNOM can be used to map the subwavelength confinement of light to a point-defect in a 2D photonic crystal microresonator. Comparison with numerical modelling shows that SNOM is able to resolve patterns in the intensity distribution that are due to the slight non-uniformity in the crystal structure. We also discuss the future possibilities for applications of different modes of SNOM to photonic crystal devices.

key words: *Photonic Crystal, Scanning Near-field Optical Microscopy, SNOM, Point Defect, Microresonator.*

1. Introduction

Photonic crystals offer exciting prospects for miniaturized optical components since, by definition, they manipulate the flow of light at dimensions less than the wavelength of light. This feature is also the source of a great challenges. Manufacturing photonic crystals requires highly accurate nanometre scale fabrication techniques. When it comes to the characterization of devices, some method for observing the interaction of light with the crystal device is required. Standard microscopy techniques are limited to a resolution of half the optical wavelength by diffraction. This is enough to resolve the light scattering out of a large crystal device, but not sufficient to resolve the detailed behaviour of the light interacting with the crystal [1].

Some groups have turned to scanning near-field optical microscopy (SNOM) as a technique for characterizing photonic crystal devices [2]–[9]. This method is not limited by diffraction. In principle it is limited only by the dimensions of the scanning probe, which can routinely be smaller than 100nm [10]. The clear advantage of SNOM, therefore, is that it offers the chance to look inside a crystal device and see where the light is going.

We begin this article, in the following section, by describing the basic principles of SNOM. In section 3 we focus on our experiments with a point defect photonic crystal microcavity where we show how SNOM can be used to map out the resonant mode of the cavity and shed light on the quality of the sample. The application of SNOM to other photonic devices is discussed in section 4 in order to highlight what possibilities SNOM has to offer future experiments with photonic crystals.

[†]Laboratory of Physical Chemistry, ETH Zurich, 8093 Zurich, Switzerland

[††]CNRS/LPN, route de Nozay, 91460 Marcoussis, France

[†††]Research Center of Crete, Heraklion, Crete, Greece

[††††]Laboratory and Department of Physics and Astronomy, Iowa State University, Ames, Iowa, 50011, USA

a) E-mail: vahid.sandoghdar@ethz.ch

2. The principles of SNOM

Scanning near field microscopy is a technique that allows one to avoid the diffraction limit of conventional optical microscopy. It was pioneered in the early 1980s by groups at IBM Zurich [11] and Cornell [12]. A regular optical microscope relies on propagating optical waves to form an image of some object of interest. The travelling waves, however, contain only a part of the full optical information on offer. Consider the imaging, with light of wavelength λ, of a sample that is composed of many spatial periods. As originally formulated by Abbé [13], travelling waves originating from the sample only contain information about spatial periods greater than $\lambda/2$. Information about smaller periods is contained in non-propagating evanescent waves on the sample surface. SNOM works by scattering these evanescent fields allowing, in limit of a perfect tip, detection of the full complement of spatial information. In reality, a typical tip used in SNOM has a size of 50–100nm, which for a wavelength of 1500nm gives a resolution better than $\lambda/15$. The essential elements of a typical 'collection-mode' SNOM setup are shown in Fig. 1. A sample is illuminated by some means and light is scattered by a scanning probe into the far field where the signal is collected. The most convenient system is to use an optical fibre tip as the scatterer. That way the signal is detected simply at the output of the fibre.

There are many possible variations on this basic collection-mode theme. Fibre tips can be coated with a metallic layer, the nature of the illumination can be changed or the SNOM signal detection may not be through the fibre. Distinct from collection-mode SNOM is the more commonly encountered 'illumination-mode' SNOM. This is, to some extent, the inverse of collection-mode SNOM. Instead of the tip scattering light into the far field, light is incident on the sample from a fibre tip with a metallic coating. The sub-wavelength aperture of the fibre tip produces

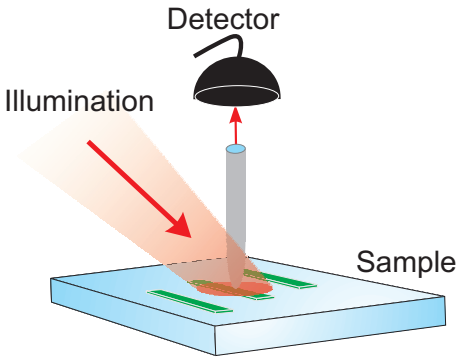

Fig. 1 SNOM: A fine tip scanned over the surface of a sample can scatter evanescent fields enabling detection of high spatial frequencies in the far-field

evanescent fields that are scattered into the far field by the sample.

An important component of any SNOM setup is the control of the tip-sample separation. If the tip is too far away, the resolution will be low owing to poor probing of the evanescent field. If the tip makes contact with the sample it will, in all likelihood, be broken. The standard technique for distance control is the 'shear-force' method [14], [15]. In this system, the tip is made to oscillate with a motion parallel to the surface. When the tip-sample distance is reduced below approximately 10 nm, a frictional force acts to damp the oscillation. Detection of the oscillation phase and amplitude can then be used to build a servo-control system to hold the tip at a fixed height above the sample. By recording the control signal of the shear-force servo one retrieves a topographical map of the sample. This is invaluable for comparison to the optical signal that is collected simultaneously with the tip. The most common system for exciting the tip motion, and the system which we use in our own experiments, is to glue a fibre tip to a quartz tuning fork [16]. These have a resonance frequency of about 32kHz. Their oscillation is conveniently excited and detected via electrodes on the fork.

3. Application of SNOM to a photonic crystal microresonator

The focus of our own work has been on point defect cavities in 2D photonic crystals. The fundamentally small nature of this microresonator is of great interest for quantum optical effects [17]–[19] because a photon confined to such tiny region carries very large electric fields. Needless to say, applications in integrated optics and analytics also welcome very small building blocks. The challenge in the design and realization of photonic crystal microresonators is to maintain the lowest volume and achieve the highest quality factor (Q) possible. Quality factors as high as a few thousand for point-defect microcavities [20], 13,000 for a 2 point defect [21] and 45,000 for a 3 point defect [22] have so far been demonstrated.

Figure 2a shows a scanning electron microscope image of a two-dimensional microresonator made of silicon. The structure has a lattice constant of $a = 1.5\mu m$, hole radius of $r = 1.3\,\mu m$ and a depth of $100\mu m$. It was fabricated by electrochemical preparation of macroporous silicon [23]–[25]. A point defect is surrounded by two pores and two waveguides that help couple light in and out of the cavity. FDTD calculations predict two sharp resonances at nominal wavelengths of $3.732\mu m$ and $3.957\mu m$ within the fundamental band gap between $3.4\mu m$ and $5.8\mu m$. Probing a photonic crystal at such mid-infrared wavelengths requires an unusual laser source. We used a cw optical parametric oscillator (OPO) that provided approximately 30mW of radiation tunable from 3.6 to 4μm. The experiment was arranged as shown in figure 2b. Radiation from the OPO was focussed onto one of the waveguides leading to the microresonator. Two SNOM probes were used in the experiment. One was a localised detector (probe #1) to monitor the output of the resonator structure [2] while the other (probe #2) was used to image the light in the resonator from the surface of the crystal [7].

Both probes consisted of uncoated fibre tips etched from fluoride glass fibre, which is suitable for work in

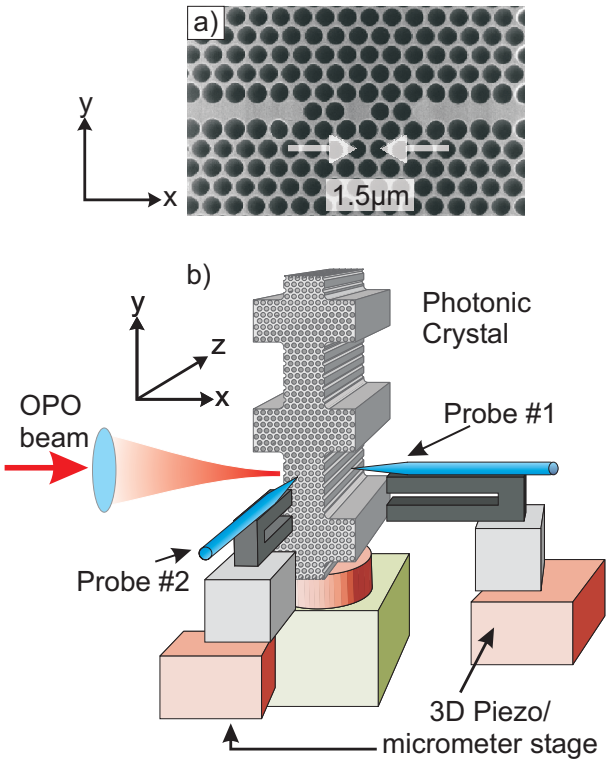

Fig. 2 a) Top view of a photonic crystal microcavity in macroporous silicon. b) Schematic of the microcavity SNOM setup. Tip #1 is used to detect light from the output waveguide while tip #2 is used to scan the surface of the crystal. The shape of the crystal was designed to aid coupling into and out of the sample [2]

the mid-infra-red. The fibre tips were glued to quartz tuning forks enabling shear force control of the tip-sample distance. In such a setup there are many mechanical degrees of freedom that must be controlled. We could adjust the position and tilt of the sample relative to the SNOM probes, while the probes themselves were mounted on combined 3D-piezo stages and 3D micrometre translation stages.

The photonic crystal in this experiment is very deep. Clearly, if the light is coupled into the crystal too deep down, probe #2 would not see any evanescent field at the surface. This means coupling in the light near the surface. This leads to a second problem, which is to discriminate between the light that passes through the sample and that which passes over the surface. This is the reason for using the SNOM tip #1 as a local detector. Figure 3a shows a sample image collected by this probe. The spot 'α' can be identified as the light that passes through the sample while the larger blob 'β' is the light passing over the sample. We note that in this configuration the tip does not exclusively measure the near-field. Nevertheless, the full width at half-maximum (FWHM) of the spot α at the exit facet is about 4 μm, corresponding to only a bit more than λ. By repeating measurements such as that shown in 3a at different laser frequencies, the resonance wavelengths of the cavity could be determined as 3.62 μm and 3.84 μm, as shown in figure 3b.

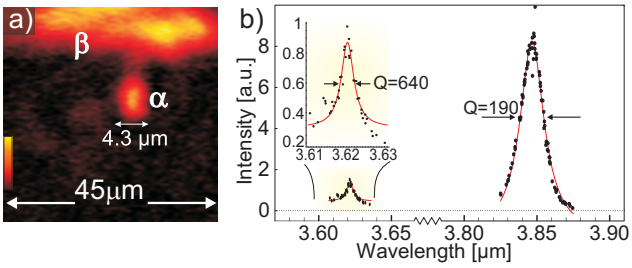

Fig. 3 a) The light emitted form the photonic crystal as measured using SNOM tip 1. b) The transmission spectrum of the point defect cavity measured using the SNOM tip 1. (Image b) taken from [2])

Before considering the experimental results from tip #2 it is worth discussing what one might hope to observe. Figures 4a and b display the intensity distribution expected for the two modes as calculated by two-dimensional FDTD simulations. The very rapid and strong intensity modulations at length scales well below a wavelength are the features that one would like to capture with SNOM. Observation of such rapid spatial modulations is limited by the size of the probe used to scatter the field. It is therefore important to consider the effect of finite tip size. Figures 4c and d show image b after a convolution with Gaussian filter functions of FWHM 500nm and 1400nm corresponding to $\lambda/7$ and $\lambda/3$ respectively. We remark that, strictly speaking, the choice of this filter is not rigorous. However, because the interaction mechanism of a SNOM tip with the sample is neither theoretically nor experimentally known in a quantitative manner, we simply convolve the intensity with a Gaussian filter function. Clearly, any coherent effects or complex polarization dependent processes are neglected in this coarse treatment. Nevertheless, this procedure is very helpful in acquiring intuitive and qualitative understanding of the system. A comparison of images b, c and d emphasizes the important role of resolution in optical microscopy.

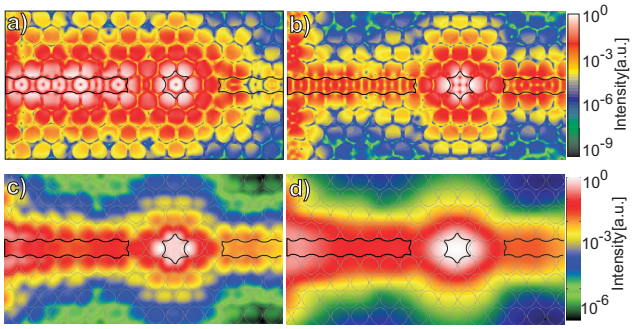

Fig. 4 a) FDTD model of the intensity of the short wavelength mode in figure 3b. b) FDTD model of the intensity of the long wavelength mode in figure 3b. c) Convolution of the model in b) with a 500nm detection window. d) Convolution of the model in b) with a 1400nm detection window. (Images a) and b) taken from [2])

We now turn to measurements made using probe #2. Figure 5b displays the topography signal of the part of the sample that is examined. The fluoride glass tips used in these experiments were extremely fragile and prone to breakage. For this reason, the probe in this run was not very sharp, leading to low lateral topography resolution. We point out that, although it is necessary to use very sharp tips for SNOM studies in the visible range, a less pointed fibre tip can still serve as a subwavelength probe for the mid-infrared regime while also providing more signal than a very fine tip. In any event, although the individual pores are not easy to recognize in figure 5b, the topography image suffices to identify the two waveguides and the point defect so that one can correlate the optical signal with the photonic crystal structure. Figure 5c shows the raw data of the optical intensity signal recorded by near-field probe #2 while the laser wavelength was tuned to the resonance at $\lambda = 3.84 \mu m$. This data was taken simultaneously with the topography signal of figure 5b which we have used together with our knowledge of the scan range to overlap the photonic crystal geometry as a guide to the eye. The propagation of light in the first waveguide and its confinement about the point defect are clearly seen.

The SNOM image in figure 5c reveals several properties that are not predicted by the FDTD simulations

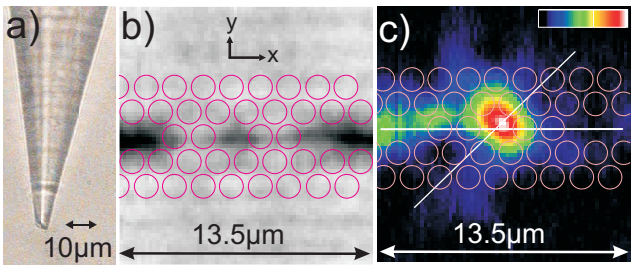

Fig. 5 a) A SNOM probe made from fluoride glass fibre. b) Topography signal from the shear-force control system. c) SNOM image taken simultaneous with b). (Images b) and c) taken from [7])

of figure 4b, c or d, independent of any resolution considerations. Firstly, the microresonator mode is tilted whereas the image in 4b shows symmetry along the x and y axes. Secondly, the light is pushed to one side by a fraction of a wavelength in the last part of the input waveguide. Thirdly, the measurements reveal subwavelength details of the intensity modulations along this waveguide which again seem to be different from that of figure 4. The intriguing possibility is that these variations are related to deviations of the structure from the ideal situation modelled in Fig. 4. Electron microscopy studies of macroporous silicon photonic crystals have shown that one might typically obtain up to 10% fluctuations in the diameters of the pores neighboring the missing pores [26]. Could these small variations lead to the asymmetry observed in Fig. 5c?

Owing to the depth of the crystal, a complete description of our system is only possible using a 3D-FDTD model. Such a model will be presented shortly. It is however instructive to apply 2D-FDTD models to gain some intuitive feeling for the important parameters that influence our system. Figures 6a, c and e show three examples of the microresonator mode from figure 4b if slight changes are made to the pores surrounding the point defect. The percentage change in pore diameter is indicated in the figures. Figures 6b, d and f display the corresponding images after the consideration of a finite SNOM resolution. Similarly, the properties of light in the waveguide can also be attributed to deviations of pore diameters surrounding the waveguide. Figure 6g-l show three examples of light propagation in structures with only two pores being 10% smaller than other holes along the waveguide. The modelling here shows two important features. Firstly, small variations in the size of the hole diameter can lead to large changes in the spatial mode of the microcavity and waveguide. Secondly, these variations are apparent even after convolution with a detection aperture. The results of these 2D-models can be used to guide the parameters to be investigated using 3D models, which take many more hours to compute.

Aside from the asymmetry of the SNOM image in figure 5c, another interesting feature is that the light intensity at the surface is very low in the output waveguide. A likely explanation has to do with the depth of the crystal. A test of this idea can be combined with the intuition gained from the 2D models to produce a 3D-FDTD model as shown in figure 7. Figure 7a shows the intensity distribution at the photonic crystal/air interface for a structure where two holes surrounding the microcavity and two holes along the input waveguide are taken to be 10% smaller than the nominal value. The intensity distribution in the yz-plane along the middle of the waveguides and the point defect is displayed in figure 7b. After interacting with the point defect the light is pushed downward in the output waveguide

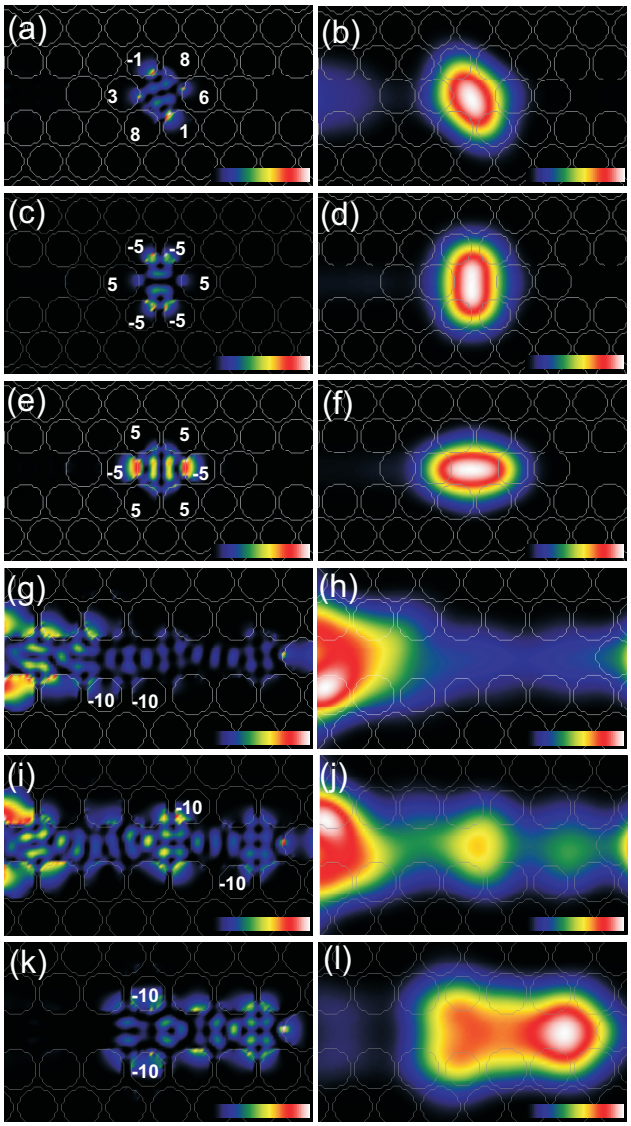

Fig. 6 Left-hand pictures show a 2D FDTD model of field intensity and the percentage change in the hole size. Right-hand pictures show the simulated measurement with a tip aperture of 1.4μm. Parameters used in this model are r/a=0.437, n=3.43 and a=1.5μm. Dimensionless frequencies, from top to bottom, are 0.3939, 0.3746, 0.3765, 0.3886, 0.3890 and 0.3931.

so that there is much less light at the surface of the photonic crystal, in agreement with our experimental observation.

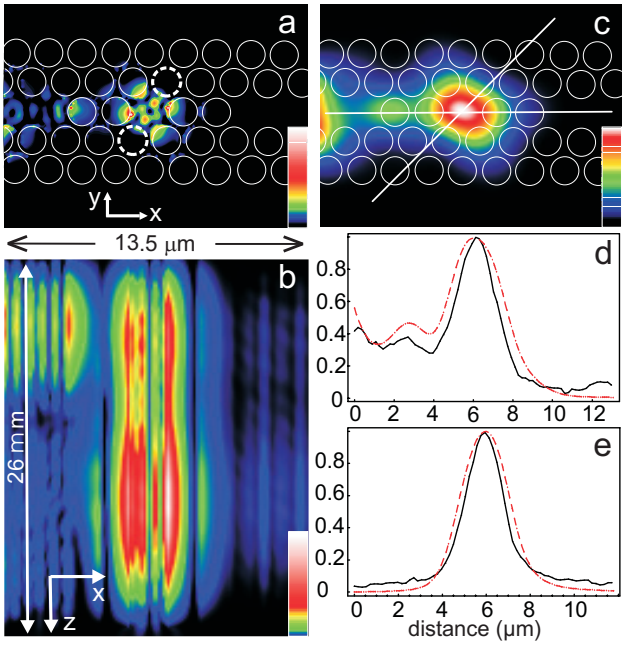

Fig. 7 a) 3D FDTD model of the field intensity at the crystal surface with indicated holes 10% smaller than nominal value and the waveguide configured as shown in figure 6g. b) 3D FDTD model of the field intensity as a function of depth through the crystal. Cross section is taken along the centre of the structure. c) Modelled intensity after convolution with 1.4μm detection window. Images d) and e) show a comparison of theoretical and experimental cross-sections along the waveguide and diagonal to the waveguide respectively. Solid is experimental data, dashed is theoretical. (From [7]).

Figure 7c plots the intensity distribution on the upper surface after convolution with a Gaussian profile of FWHM 1.4μm corresponding to about $\lambda/3$. The outcome shows good qualitative agreement with figure 5c. The mode is clearly tilted, there are intensity modulations in the waveguide and there is no significant amount of light in the second waveguide. The quantitative agreement between the two becomes clear in figures 7d and 7e where we plot two cross-sections corresponding to those shown in figures 7c and 5c. We do not claim that through this model we have determined the exact structure of the microcavity. Clearly, not all aspects of the experimental observations could be recovered. For example, the deflection of light to one side by a few hundred nanometers is not reproduced, the tilt angle of the mode is not identical to the SNOM image, and a small intensity asymmetry within the microcavity spot remains unexplained. At any rate, the configurations we have considered using 3D modelling are far from exhaustive and there is no guarantee that a given optical pattern corresponds to a unique cavity configuration. What we can say is that SNOM is a sensitive investigative tool for examining the impact of imperfect fabrication on the light propagation through a photonic crystal defect. Improvements in resolution and 3D modelling will improve the ability of SNOM to identify the details of photonic crystal devices.

4. Advanced SNOM: Beyond intensity measurement

Our results show how a sub-wavelength scale probe can be used to image the intensity of a light field in a photonic crystal. This is the most obvious and intuitive way to use SNOM. There are, however, some other more advanced methods that can be applied to SNOM systems that provide extra information. Their application to photonic crystals would provide even more information about the nature of such devices.

There have been several SNOM experiments carried out on silica microspheres [27]–[30]. The whispering gallery modes (WGMs) of these spheres have an extraordinarily high quality factor of up to 10^{10} [31]. The free spectral range of such a system is typically in the range of a few hundred gigahertz. Within a free spectral range there are many non-degenerate WGMs typically separated by a few gigahertz. Owing to the large free-spectral-range and limited tunability of the lasers used to probe such spheres, it is often impossible to map out the full mode structure of the WGMs, especially given that the exact nature of each sphere is determined by the unique geometry imparted during the manufacturing process. Götzinger *et al.* have used SNOM to provide a spatio-spectral map of the WGMs [30] allowing the identification of WGMs via the shape of the evanescent field on the surface of the microsphere. This combination of spectroscopy and microscopy could be a powerful tool for investigating photonic crystal devices. For example, the modulations in a line-defect waveguide measured as function of frequency and space would give insight into the dispersion of the light propagating in the waveguide.

A second system that would be interesting if applied to photonic crystal devices is heterodyne-SNOM. In this system, the SNOM signal is passed to an interferometer where it is mixed with a frequency shifted reference beam [32]–[36]. The demodulation of the interferometer output allows access to both the optical phase and amplitude of the light detected by the SNOM probe. The particular example of this system that has the most relevance for photonic crystal work is that of Balistreri *et al.* [35]. Here the modes of a ridge waveguide were measured using heterodyne-SNOM with the results showing rich behaviour of the optical phase, including phase singularities. An extension to this system was the combination with a femtosecond pulsed laser. By shifting the path length of the reference beam is was possible to track the propagation of the pulse through

the waveguide [36]. Both these ideas promise to reveal much about the properties of photonic crystal devices, just as they did for the ridge waveguides.

A third line of experiments that might be possible with SNOM techniques is the active control of photonic crystal devices. One could imagine using a high index probe, similar to that of the crystal medium, to create or modify defects on demand. In this way, active switching and control of the photonic crystal devices would be possible. The effect of a SNOM probe was actually visible in some of the experiments with silica microspheres. The resonant frequency of the WGMs was seen to shift when a large tip (1μm) was applied to the WGMs [30].

A fourth possibility for advanced SNOM is to place an emitter at the end of the SNOM probe. It has previously been demonstrated that a single molecule or diamond colour centre can be used as an active light source for illumination-mode SNOM measurements [37], [38]. Such a system would be intriguing if applied to a high-Q, low-volume photonic crystal microresonator, such as those made by Srinivasan *et al.* [21] and Akahane *et al.* [22]. An emitter coupled to such a cavity could be used for cavity-QED experiments [18] with the added advantage that the position of the emitter within the cavity can be accurately controlled. Measuring the fluorescence lifetime of the emitter as a function of position in and around the cavity would enable mapping of the local density of states. The same technique could potentially be applied to a pure photonic crystal. The local density of states is predicted to vary as a function of position in a crystal [39]. Through variations of the excited state lifetime of an emitter, these variations could be measured.

5. Conclusion

When it comes high resolution imaging the flow of light in a photonic crystal, near field microscopy is not just a useful technique, it is the only technique. Far field microscopy is limited by diffraction and therefore cannot reveal the details of light intensity over the sub-wavelength dimensions that are relevant in photonic crystal systems. Numerous groups are now applying SNOM to photonic crystals for just this reason.

Our experiments using SNOM on a point defect microcavity show how the detailed, sub-wavelength behaviour of the optical intensity can provide clues to structure and quality of photonic crystal devices. We have observed a rotation in the shape of a resonant mode of our cavity and shown that such rotation is easily explained by the expected fabrication tolerances of such devices. This highlights the sensitivity of photonic crystal devices to small fabrication errors

The application of SNOM to photonic crystal devices is in its infancy. There are many modes of operation that have been demonstrated on other photonic systems that, if applied to photonic crystals, could provide a wealth of information.

Acknowledgements

We are grateful to Albert Birner, Ralf Wehrspohn, Frank Müller and Ulrich Gösele for the fabrication of photonic crystal samples. Our work has been generously supported by the Deutsche Forschungsgemeinschaft (DFG).

References

[1] M. Lončar, D. Nedeljković, T. P. Pearsall, J. Vučković, A. Scherer, S. Kuchinsky, and D. C. Allan. Experimental and theoretical confirmation of bloch-mode light propagation in planar photonic crystal waveguides. *Appl. Phys. Lett.*, 80(10):1689–1691, 2002.

[2] P. Kramper, A. Birner, M. Agio, C. M. Soukoulis, F. Müller, U. Gösele, J. Mlynek, and V. Sandoghdar. Direct spectroscopy of a deep two-dimensional photonic crystal microresonator. *Phys. Rev. B*, 64:233102–1–4, 2001.

[3] S. I. Bozhevolnyi, V. S. Volkov, J. Arentoft, A. Boltasseva, T. Søndergaard, and M. Kristensen. Direct mapping of light propagation in photonic crystal waveguides. *Opt. Commun.*, 212(1-3):51–55, 2002.

[4] S. I. Bozhevolnyi, V. S. Volkov, T. Søndergaard, A. Boltasseva, P. I. Borel, and M. Kristensen. Near-field imaging of light propagation in photonic crystal waveguides: Explicit role of bloch harmonics. *Phys. Rev. B*, 66(23):235204, 2002.

[5] D. Gerard, L. Berguiga, F. de Fornel, L. Salomon, C. Seassal, X. Letartre, P. Rojo-Romeo, and P. Viktorovitch. Near-field probing of active photonic-crystal structures. *Opt. Lett.*, 27(3):173–175, 2002.

[6] Dong-Jae-Shin, Se-Heon-Kim, Jeong-Ki-Hwang, Han-Youl-Ryu, Hong-Gyu-Park, Dae-Sung-Song, and Yong-Hee-Lee. Far- and near-field investigations on the lasing modes in two-dimensional photonic crystal slab lasers. *IEEE J. Quantum Elect.*, 38(7):857–866, 2002.

[7] P. Kramper, M. Kafesaki, C. M. Soukoulis, A. Birner, F. Müller, R. Wehrspohn, U. Gösele, J. Mlynek, and V. Sandoghdar. Near-field visualization of light confinement in a photonic crystal microresonator. *To appear in Opt. Lett.*, 2003.

[8] E. Flück, N. F. van Hulst, W. L. Vos, and L. Kuipers. Near-field optical investigation of three-dimensional photonic crystals. *Phys. Rev. E*, 68(1):15601(R), 2003.

[9] K. Okamoto, M. Lončar, T. Yoshie, A. Scherer, Y. M. Qiu, and P. Gogna. Near-field scanning optical microscopy of photonic crystal nanocavities. *Appl. Phys. Lett.*, 82(11):1676–1678, 2003.

[10] M. A. Paesler and Moyer P. J. *Near-Field Optics: Theory, Instrumentation, and Applications.* Wiley-Interscience, 1997.

[11] D. W. Pohl, W. Denk, and M. Lanz. Optical stethoscopy: Image recording with resolution $\lambda/20$. *Appl. Phys. Lett.*, 44(7):651–653, 1984.

[12] A. Lewis, M. Isaacson, A. Harootunian, and A. Muray. Development of a 500 å spatial resolution light microscope. *Ultramicroscopy*, 13:227–232, 1984.

[13] E. Abbe. *Gesammelte Abhandlungen*, volume 2. G. Fischer Verlag, Jena, 1906.

[14] R. Toledo-Crow, P. C. Yang, Y. Chen, and M. Vaez-Iravani. Near-field differential scanning optical microscope with atomic force regulation. *Appl. Phys. Lett*, 60(24):2957–

2959, 1992.

[15] E. Betzig, P. L. Finn, and J. S. Weiner. Combined shear force and near-field scanning optical microscopy. *Appl. Phys. Lett*, 60(20):2484–2486, 1992.

[16] K. Karrai and R. D. Grober. Piezoelectric tip-sample distance control for near field optical microscopes. *Appl. Phys. Lett.*, 66(14):1842–1844, 1995.

[17] H.J. Kimble. Strong interactions of single atoms and photons in cavity qed. *Physica Scripta*, T76:127–137, 1998.

[18] J. Vučković, M. Lončar, H. Mabuchi, and A. Scherer. Design of photonic crystal microcavities for cavity qed. *Phys Rev. E*, 65(1):016608, 2002.

[19] J. Vučković and Y. Yamamoto. Photonic crystal microcavities for cavity quantum electrodynamics with a single quantum dot. *Appl. Phys. Lett*, 82(15):3274, 2003.

[20] T. Yoshie, J. Vučković, A. Scherer, Hao Chen, and Dennis Deppe. High quality two-dimensional photonic crystal slab cavities. *Appl. Phys. Lett.*, 79(26):4289–4291, 2001.

[21] K. Srinivasan, P. E. Barclay, O. Painter, J. Chen, A. Y. Cho, and C. Gmachl. Experimental demonstration of a high quality factor photonic crystal microcavity. *Appl. Phys. Lett.*, 83(10):1915–1917, 2003.

[22] Y. Akahane, T. Asano, B.-S. Song, and S. Noda. High-Q photonic nanocavity in a two-dimensional photonic crystal. *Nature*, 425(6961):944, 2003.

[23] V. Lehmann. The physics of macropore formation in low doped n-type silicon. *J. Electrochem. Soc.*, 140(10):2836–2843, 1993.

[24] A. Birner, U. Grüning, S. Ottow, A. Schneider, F. Müller, V. Lehmann, H. Föll, and U. Gösele. Macroporous silicon - a two-dimensional photonic bandgap material suitable for the near-infrared spectral range. *Phys. Stat. Sol. A*, 165(1):111, 1998.

[25] J. Schilling, R. B. Wehrspohn, A. Birner, F. Müller, R. Hillebrand, U. Gösele, S. W. Leonard, J. P. Mondia, F. Genereux, H. M. van Driel, P. Kramper, V. Sandoghdar, and K. Busch. A model system for two-dimensional and three-dimensional photonic crystals: macroporous silicon. *J. Opt. A: Pure Appl. Opt.*, 3(6):S121–S132, 2001.

[26] A. Birner. PhD thesis, Martin-Luther University at Halle-Wittenberg, 2000.

[27] J. C. Knight, N. Dubreuil, V. Sandoghdar, J. Hare, V. Lefèvre-Seguin, J. M. Raimond, and S. Haroche. Mapping whispering-gallery modes in microspheres with a near-field probe. *Opt. Lett.*, 20(14):1515–1517, 1995.

[28] J. C. Knight, N. Dubreuil, V. Sandoghdar, J. Hare, V. Lefevre-Seguin, J. M. Raimond, and S. Haroche. Characterizing whispering-gallery modes in microspheres by direct observation of the optical standing-wave pattern in the near field. *Opt. Lett.*, 21(10):698–700, 1996.

[29] S. Götzinger, S. Demmerer, O. Benson, and V. Sandoghdar. Mapping and manipulating whispering gallery modes of a microsphere resonator with a near-field probe. *J. Microsc.*, 202(1):117–121, 2001.

[30] S. Götzinger, O. Benson, and V. Sandoghdar. Towards controlled coupling between a high-Q whispering-gallery mode and a single nanoparticle. *Appl. Phys. B*, 73(8):825–828, 2001.

[31] M. L. Gorodetsky, A. A. Savchenkov, and V. S. Ilchenko. Ultimate Q of optical microsphere resonators. *Opt. Lett.*, 21(7):453–457, 1996.

[32] M. Vaez-Iravani and R. Toledo-Crow. Phase contrast and amplitude pseudoheterodyne interference near field scanning optical microscopy. *Appl. Phys. Lett.*, 62(10):1044–1046, 1993.

[33] J.N. Walford, K.A. Nugent, A. Roberts, and R.E. Scholten. Three-dimensional phase imaging with a scanning optical-fiber interferometer. *Appl. Opt*, 38(16):3508–3515, 1999.

[34] P. L. Phillips, J. C. Knight, J. M. Pottage, G. Kakarantzas, and J. St. P. Russell. Direct measurement of optical phase in the near field. *Appl. Phys. Lett.*, 76(5):541–543, 2000.

[35] M. L. M. Balistreri, J. P. Korterik, L. Kuipers, , and N. F. van Hulst. Local observations of phase singularities in optical fields in waveguide structures. *Phys. Rev. Lett*, 85(2):294–297, 2000.

[36] M. L. M. Balistreri, H. Gersen, J. P. Korterik, L. Kuipers, and N. F. van Hulst. Tracking femtosecond laser pulses in space and time. *Science*, 294(5544):1080–1082, 2000.

[37] J. Michaelis, C. Hettich, J. Mlynek, and V. Sandoghdar. Optical microscopy using a single-molecule light source. *Nature*, 405(6784):325–327, 2000.

[38] S. Kühn, C. Hettich, C. Schmitt, J.-Ph. Poizat, and V. Sandoghdar. Diamond colour centres as a nanoscopic light source for scanning near-field optical microscopy. *J. of Microscopy*, 202(1):2–6, 2001.

[39] T. Susuki and P. K. L. Yu. Emission power of an electric dipole in the photonic band structure of the fcc lattice. *J. Opt. Soc. Am. B*, 12(4):570, 1995.